

# Lawrence Berkeley National Laboratory

## Lawrence Berkeley National Laboratory

### **Title**

A method to attenuate U(VI) mobility in acidic waste plumes using humic acids

### **Permalink**

<https://escholarship.org/uc/item/76f3m465>

### **Author**

Wan, J.

### **Publication Date**

2011-03-20

Peer reviewed

## **A Method to Attenuate U(VI) Mobility in Acidic Waste Plumes Using Humic Acids**

Jiamin Wan\*, Wenming Dong, Tetsu K. Tokunaga

Earth Sciences Division, Lawrence Berkeley National Laboratory,

1 Cyclotron Road, Berkeley, California 94720

510-486-6004 (phone), 510-486-7152 (fax)

[jwan@lbl.gov](mailto:jwan@lbl.gov)

**Abstract.** Acidic uranium (U) contaminated plumes have resulted from acid-extraction of plutonium during the Cold War and from U mining and milling operations. A sustainable method for in-situ immobilization of U under acidic conditions is not yet available. Here, we propose to use humic acids (HAs) for in-situ U immobilization in acidic waste plumes. Our laboratory batch experiments show that HA can adsorb onto aquifer sediments rapidly, strongly and practically irreversibly. Adding HA greatly enhanced U adsorption capacity to sediments at pH below 5.0. Our column experiments using historically contaminated sediments from the Savannah River Site under slow flow rates (120 and 12 m/y) show that desorption of U and HA were non-detectable over 100 pore-volumes of leaching with simulated acidic groundwaters. Upon HA-treatment, 99% of the contaminant [U] was immobilized at  $\text{pH} < 4.5$ , compared to 5% and 58% immobilized in the control columns at pH 3.5 and 4.5, respectively. These results demonstrated that HA-treatment is a promising in-situ remediation method for acidic U waste plumes. As a remediation reagent, HAs are resistant to biodegradation, cost effective, nontoxic, and easily introducible to the subsurface.

## Introduction

Plumes of uranium (U) contamination in groundwaters have resulted from mining, ore milling, and various nuclear energy and weapons production processes. In several U.S. Department of Energy (DOE) weapon facilities including the Savannah River Site (SRS), Oak Ridge Site (ORS), and the Hanford Site, acidic waste solutions containing low-level radionuclides were discharged into unlined seepage basins for decades. As the results, acidic waste plumes developed in groundwater underneath the basins. After years of costly remediation efforts U concentrations remain 10 to 1,000 times higher than its maximum contaminant levels (MCL = 0.13  $\mu\text{M}$ ), and groundwaters remain acidic with pH values as low as 3.0. A sustainable U biogeochemical remediation method has not yet been developed, especially for acidic conditions. Bioreduction-based U stabilization requires permanent maintenance of reducing conditions through indefinite supply of electron donor (1-3), and when applied in acidic plumes expensive neutralization pretreatment is required (4). Methods based on precipitation of phosphate minerals cannot keep U concentrations below its MCL at any pH, unless dissolution is kinetically controlled or phosphate is maintained at much higher concentrations than the sub- $\mu\text{M}$  levels typically found in groundwaters (5). Precipitating of uranyl vanadates can lower U to below its MCL (5), but this approach is only effective at near-neutral pH. Thus, there remains an urgent need for developing a sustainable method to remediate or attenuate the contaminant U in acidic waste plumes.

Humic substances in terrestrial and aquatic environments (6, 7) have complex properties and consist of a variety of organic components including humic acid (HA) and fulvic acid (FA). Compared to FA, HA consists of relatively higher molecular weight compounds, and has a stronger affinity toward mineral surfaces (7-10). HA is capable of interacting with contaminant

U in many ways, and greatly influences the adsorption and mobility of U in aquifer environments (9, 11-14). The influence of HA on U behavior is largely pH dependent. Under acidic pH, HA strongly adsorbs onto mineral surfaces (10, 15, 16), and the adsorbed HA in turn complexes and immobilizes contaminant metal ions such as  $\text{UO}_2^{2+}$ ,  $\text{Cu}^{2+}$ ,  $\text{Cd}^{2+}$  (9, 17-19). At neutral and slightly alkaline pH conditions, HA adsorption on the mineral surfaces becomes weaker and the HA in aqueous solution form complexes or colloids with U(VI) that enhance mobility of U(VI) (11, 18, 20, 21). Tipping et al. (23) suggested that new and high-affinity metal complexation sites are created when HA adsorbed to goethite. Because HAs are products of microbial degradation of dead plants and organisms, they are very resistant to further biodegradation (6, 24).

Building on the rich literature addressing properties of HAs, their mechanisms for sorption onto mineral surfaces, and their complexation of metals, this work is unique in proposing and testing the use of HAs to in-situ immobilize contaminant U(VI) within acidic plumes. To the best of our knowledge, this has not previously been done. Through a set of systematic equilibrium batch experiments and column HA-treatment and groundwater leaching tests on historically U contaminated sediments under environmentally relevant plume flow and chemistry conditions, we demonstrate that HA-treatment is a promising method for U remediation in acidic plumes.

## **Materials and Methods** (more details provided in Supporting Information (SI))

**Humic Acids and Stock Solutions.** A standard Soil HA (Elliott) and a reference Peat HA (Pahokee) from the International Humic Substances Society were used and their chemical properties are summarized in Table S-1 in SI. Most of the experiments were conducted using Soil HA after we found that the Peat HA has similar effect. HA stock solutions were prepared by

dissolving weighed amounts of HA in deionized water, adjusting pH to 6.5, and filtering through a 0.2  $\mu\text{m}$  filter.

**Sediments, goethite, kaolinite, and their stock suspensions.** Two sediment samples from the SRS F-Area were selected: uncontaminated background sediment (FAW-1) for batch experiments and contaminated sediment (FAW-2) for column experiments. The two sediments are within the same stratum and composed of the same minerals, predominantly quartz, kaolinite and goethite. FAW-1 and FAW-2 contain 13.0% and 5.2% of fine fraction ( $< 45 \mu\text{m}$ ), and have BET  $\text{N}_2$ -specific surface areas 4.6 and 1.9  $\text{m}^2/\text{g}$  for the whole sediment, and 35.9 and 36.5  $\text{m}^2/\text{g}$  for the fine fraction, respectively. Because the BET data showed that nearly 100% of surface areas of the bulk sediments were contributed by the fine-fractions ( $< 45 \mu\text{m}$ ), we chose to use the fine-fraction only for all the batch equilibrium adsorption studies. The bulk sediment samples were used for the column experiments. The fine-fraction ( $< 45 \mu\text{m}$ ) was also separated from the ORS background sediment (25). In addition, pure goethite and kaolinite (Alfa Aesar) were used as model systems and their BET  $\text{N}_2$ -specific surface areas are 16.2 and 20.7  $\text{m}^2/\text{g}$ , respectively. The contaminated sediment FAW-2 contained  $2.6 \pm 0.1 \text{ mg/kg U}$  in the whole sediment, and  $3.26 \pm 0.04 \mu\text{M [U]}$  in its extracted pore water with pH 4.0. Prior to the batch adsorption experiments, the fine-fractions of SRS and ORS sediments, goethite and kaolinite were suspended in deionized water as stock suspensions (25 g/L). Other chemicals used were all ACS reagent grade or higher.

**Experimental Methods.** Unless noted otherwise all batch experiments were conducted in duplicate under atmospheric pressure ( $P_{\text{CO}_2} = 10^{-3.5} \text{ atm}$ ) and room temperature (22  $^\circ\text{C}$ ). All solutions contained 0.01 M  $\text{NaNO}_3$ . The solid (sorbent) to water ratio was 5g/L. The batch reaction time was three days (based on the kinetic study), with continuous agitation on a shaker.

The vials were opened to air daily to maintain equilibrium with atmospheric CO<sub>2</sub>. The pH values were monitored and readjusted daily with small amount of 0.1 M HNO<sub>3</sub> or 0.1M NaOH solutions to ±0.05 of the target values. Aqueous U(VI) concentrations were measured with a kinetic phosphorescence analyzer (KPA-11) or ICP-MS. HA concentrations were measured using a UV-UV-Vis spectrophotometer or a Shimadzu TOC analyzer. **(1) HA and U adsorption kinetics:** four batch kinetic experiments were conducted at pH 3.5 and pH 5.0, using the SRS fine-fraction including HA adsorption, U adsorption, U adsorption onto HA pre-treated sediment, and U adsorption by amending HA into U pre-equilibrated sediment. **(2) HA adsorption capacity and reversibility:** HA adsorption capacity was investigated using a wide range of HA concentrations (10–300 mg/L) at pH 3.5, 4.5 and 5.5 for the SRS fine-fraction, and at pH = 3.5 for three different sorbents (SRS fine-fraction, goethite and kaolinite). HA desorption experiments were carried out at the end of adsorption procedure and the details are presented in SI. **(3) Effect of HA treatment on U adsorption under varied pH conditions:** U adsorption onto the SRS and ORS fine-fractions, goethite, and kaolinite were performed under varied pH (3.0–9.5), constant total U (1 µM), in the absence and presence of total 50 mg/L Soil HA and Peat HA separately. **(4) Testing HA treatment as an in-situ remediation method:** four columns were packed with historically contaminated SRS bulk sediment. Two pH conditions, 3.5 and 4.5, were tested. Under each pH condition, there were two columns; one column was treated with HA and another (control) without HA. The columns (10.0 cm tall and 2.54 cm inside diameter) were packed with the wet sediment to a bulk density 1.69 g/cm<sup>3</sup> and porosity of 0.36. During the treatment stage, 160 mL, equal to 7.9 pore volume (PV) of four different solutions, all containing 0.01 M NaNO<sub>3</sub>, with or without 500 mg/L Soil HA, at pH 3.5 or 4.5, were injected from the bottoms of vertically oriented columns. The pore water velocity was set to 120 m/yr based on the estimated

groundwater average flow rate of 120 -150 m/y in the plume region the Savannah River F-Area). After 7.9 PV of HA solution injection, the flow direction was reversed by inverting the columns. Thereafter, all columns were leached with HA-free simulated groundwater (0.01M NaNO<sub>3</sub>) with pH 3.5 or pH 4.5. At PV 60, the flow rate was slowed to 12 m/yr to increase the solution-mineral contact time and to amplify the chemical reaction signatures. The effluent solutions were analyzed for U, HA, and pH.

## Results and Discussion

**HA and U adsorption kinetics.** The rate and extent of HA and U adsorption onto the SRS sediment were measured, and the data are presented in Figure 1. The data were fit to the integrated pseudo-first-order rate equation (shown as solid and dashed lines in Figure 1). The detailed kinetic rate equations and simulated rate constants are presented in Table S-3 in SI. The data in Figure 1a show that HA adsorption onto the sediment is a rapid and pH-dependent process. HA quickly reached ~100% adsorption within one minute at pH 3.5, and about 2 hours at pH 5.0. The fitted first order constant for the adsorption process is  $344 \pm 55 \text{ h}^{-1}$  and  $183 \pm 28 \text{ h}^{-1}$  at pH 3.5 and 5.0, respectively. U adsorption onto the sediment without HA (Figure 1b), required ~10 hour to reach equilibrium, and ~22% and ~86% adsorption of the original  $1.0 \mu\text{M}$  [U] was achieved under pH 3.5 and 5.0, respectively. However, the addition of HA (Figure 1c and 1d) significantly enhanced the rate and extent of U adsorption onto the sediment, regardless of whether HA was added before (Figure 1c) or after (Figure 1d) the U was added. This rapid adsorption suggests strong binding forces between U and the HA-altered grain surfaces. The fitted first order U adsorption rate increased from  $0.84 \text{ h}^{-1}$  to  $145 \text{ h}^{-1}$  at pH 3.5, and  $112 \text{ h}^{-1}$  to  $1082 \text{ h}^{-1}$  at pH 5.0. The HA-treatment largely increased the extent of U adsorption, from 22% to



96% at pH 3.5, and 86% to ~100% at pH 5.0. Note that ~100% aqueous U adsorption was not achieved at pH 3.5 in this experiment, but we believe that a treatment with higher HA (> 50 mg/L) could achieve ~100% adsorption of U at pH 3.5, and thus determination of HA adsorption capacity (isotherms) is necessary.

**HA Adsorption Capacity and Reversibility.** The data on HA adsorption capacity onto the SRS fines are presented in Figures 2a and 2c; and the data comparing HA sorption onto three different sorbents are shown in Figures 2b and 2d. The maximum (~100%) adsorption onto the SRS fines (Figure 2a) was reached for initial [HA] of 50, 100, and 200 mg/L at pH 5.5, 4.5, and 3.5, respectively. Comparing HA adsorption onto three different sorbents at pH 3.5 (Figure 3b), the adsorption capacity (mass basis) followed the order of SRS fines > goethite > kaolinite. To understand the HA adsorption capacity based on their specific surface areas, HA adsorption were transformed into surface area normalized adsorption isotherms (Figure 2c-d). All adsorption isotherms show a steep initial slope at low HA concentrations and then reach a plateau as the equilibrium concentration increases. The results indicate the presence of finite adsorption sites for each sorbent surface, and the HA adsorption can be described by the Langmuir Equation (solid lines in Figure 2c-d). The fitted Langmuir parameters are presented in Table S-4 in SI. The values of the maximum adsorption capacity ( $Q_{\max}$ ) of HA onto the SRS fine-fraction are  $1.24 \pm 0.05 \text{ mg/m}^2$ ,  $0.76 \pm 0.020 \text{ mg/m}^2$ , and  $0.46 \pm 0.040 \text{ mg/m}^2$  at pH 3.5, 4.5, and 5.5, respectively. Goethite shows significantly greater adsorption capacity ( $2.42 \pm 0.11 \text{ mg/m}^2$ ) than SRS fine-fraction ( $1.24 \pm 0.05 \text{ m}^2/\text{g}$ ) and kaolinite ( $1.00 \pm 0.018 \text{ mg/m}^2$ ). The reversed order of adsorption capacity between SRS fine-fraction and goethite shown in Figure 2d vs. 2b reflects the difference between their specific surface areas:  $35.9 \text{ m}^2/\text{g}$  for SRS fines and  $16.2 \text{ m}^2/\text{g}$  for the goethite used in this study

The reversibility of adsorbed HA was investigated through desorption experiments. We observed that HA desorption is very limited ( $< 0.5\%$  of total adsorbed) under all experimental conditions using the same pH background solution without HA. This is an indication that, besides the electrostatic interactions, the inner-sphere surface complexes of HA with the sorbents are formed that makes the adsorbed HA stable under acidic and slightly acidic conditions. These observations are consistent with results reported in the literature (9, 10, 16, 18, 29). Such strong adsorption of HA on mineral surfaces results in strong desorption hysteresis (irreversibility).

**Effect of HA-addition on U Adsorption under Varied pH Conditions.** The data of pH-dependent U adsorption onto four different sorbents are presented in Figures 3 a-d, respectively. The three curves in each figure present data from three conditions: the absence of HA, the presence of Soil HA, and Peat HA, respectively. Overall, HA addition greatly increased the extent of U adsorption within the region of  $\text{pH} < 5.0$ . HA adsorption onto SRS fines increased from  $\sim 10\%$  without HA to  $\sim 85\%$  with both types of HA at pH 3.0 and from  $\sim 50\%$  to  $\sim 100\%$  at pH 4.0. The HA enhanced U adsorption was also observed with all the other sorbents under acidic conditions. Note that  $\sim 100\%$  U adsorption could have been achieved under  $\text{pH} \leq 3.5$ , if a higher HA concentration ( $> 50 \text{ mg/L}$ ) was applied to overcome proton competition. The HA concentration used in this experiment,  $50 \text{ mg/L}$ , was only  $\sim 22\%$  of the HA adsorption capacity ( $Q_{\text{max}}$ ) on SRS fines at pH 3.5 (Figure 2c). Another observation is that HA addition decreased U adsorption at neutral and alkaline pH conditions, which is consistent with the results reported in literature (11, 18, 20, 21). This decreased U adsorption can be explained by the decreased HA adsorption onto solids with increasing pH shown in Figure S-1 in SI. The dissolved HA formed aqueous U-HA complexes at neutral and slightly alkaline conditions, restricting the extent of U adsorption onto the grain surfaces. Figure S-2 in SI shows that HA-

bounded U is predicted to be the dominant U species under  $\text{pH} < \sim 7.5$ , and carbonate-bounded U become dominant at  $\text{pH} > \sim 7.5$ . The decreased U adsorption at  $\text{pH} > \sim 7.5$  is due to competition between dissolved HA, carbonate, and U-carbonate complexes for adsorption onto surface sites, where observed HA adsorption remains high at pH up to 9.5, particularly for SRS sediment and goethite (Figure S-1). Kaolinite features point of zero charge (PZC) at around pH 5 (18, 22). Kaolinite becomes negatively charged at higher pH, causing decreased HA adsorption because of electrostatic repulsion with negatively charged HA, and further resulting in decrease of U adsorption with increasing pH (Figure 3d). However, goethite and goethite-rich SRS fine-fraction possess positively charged surfaces at pH up to  $\sim 9.0$  (PZC) (10, 27, 28) that favor HA adsorption. Soil HA and Peat HA showed similar impacts on U adsorption onto the sorbents except for kaolinite. This difference (Figure 3d) can be explained by the fact that kaolinite surfaces prefer HA with higher molecular weight (30, 31). In summary, these results demonstrate that HA treatment at moderate concentrations can significantly enhance U(VI) adsorption to natural sediments, and provide the basis for our proposed method of using HA to immobilize U in acidic ( $\text{pH} < 5.0$ ) waste plumes.

**Testing HA Treatment as an in-situ U Remediation Method.** The measured [HA], pH, and [U] values in effluents from column experiments are presented in Figure 4. The first vertical dashed-lines indicate the transition point of the two stages: HA treatment/injection and simulated groundwater leaching/desorption. The two control columns experienced the same processes under the same conditions except that the influent solutions did not contain HA. At PV 60 (the second set of dashed-lines) the flow rates were changed from 120 m/yr to 12 m/yr.

**Effluent HA.** The HA breakthrough curves from the two HA-injected columns are presented in Figures 4a-b. HA breakthrough occurred at PV  $\sim 6$  and PV  $\sim 4$  for the pH 3.5 and 4.5

columns, respectively. This result is consistent with the batch HA adsorption result (Figure 2) in that the adsorption capacity of HA is higher at lower pH. After stopping HA injecting, the columns were turned upside down, inflow lines were reconfigured to reverse the flow direction (relative to the original column coordinates), and the influent solution was changed to simulated groundwater (0.01M NaNO<sub>3</sub>) with corresponding pH 3.5 or 4.5 to leach U. The high HA peaks occurred at PV  $\approx$  7.7 as the results of groundwater displacing the free HA-containing pore water from stage one. The HA concentrations quickly decreased to near and below the detection limit (0.5 mg C/L for the TOC analyzer and 0.5 mg HA /L for UV-vis spectrophotometer), and the effluent [HA] remained at this low level for the entire leaching stage, indicating that desorption of HA is negligible. An important observation is that the adsorbed HA remained adsorbed as effluent pH increased up to 6.0 (see pH curves in Fig.4d). The total HA injected is  $\sim$ 80 mg for each HA-treated column, and the measured total HA loss in effluents is  $\sim$ 1.2 mg and  $\sim$ 4.2 mg for the pH 3.5 and 4.5 columns, respectively. Relative to the measured maximum HA adsorption capacity on SRS fine-fraction of 206 mg at pH 3.5 and 126 mg at pH 4.5, the total adsorbed HA accounts for 40% and 60% of the adsorption capacity of the column sediments at each pH condition.

***Effluent pH.*** The sediment used to pack the columns has the original pore-water pH = 4.0. The effluent pH values are presented in Figures 4c-d. During stage one, the effluent pH values varied between 4.0 and 5.0, irrespective of influent pH, with or without HA. This initial pH response indicated sediment-solution reactions that consumed the injected protons to different degrees. At the beginning of stage two, the effluent pH values reflected the influent pH values of 3.5 and 4.5 because of the reversed flow direction, except for the pH 4.5 control column (Figure 4d; we do not have an explanation for the increased pH at the point of flow

direction reversal). The pH quickly increased, reached maximum values at PV  $\approx$  15. Thereafter the pH values gradually decreased and became equal and slightly higher than the influent pH values at about PV 35 and PV 45 for influent pH 3.5 and pH 4.5, respectively. At PV 60, the flow rate was reduced by a factor of 10, which again resulted in increases of effluent pH values. The two pH peak-values at PV around 78 and 99 correspond to times when the pump was stalling (suggesting that the rate of proton consumption became greater than that of supply by the flow), although a quantitative understanding of the proton consumption reaction is beyond the scope of this paper. The important pH information we gained from this experiment is that although pH varied from 3.5 to 6.0, the increased pH did not impact either HA adsorption or U trapping for HA-treated sediments.

***U Release.*** Uranium breakthrough curves are presented in Figures 4e-f. The high effluent [U] concentrations from all the columns at the beginning of stage 1 reflect the [U] in displaced original sediment pore-water (1.1 to 1.4  $\mu$ M). The [U] decreased as the flow continued, and decreased more rapidly for the HA-injecting columns. The local variations in effluent [U] during stage 1 as well as early stage 2 resulted from two causes. The high effluent [HA] in HA-treated columns correlated with increased [U] in the vicinity of the stage 1 to 2 transitions, attributing to U mobilization through aqueous HA complexes. The other cause is the pH fluctuation for the two control columns; increased pH corresponded to decreased effluent [U]. Nevertheless, upon switching to the leaching stage, [U] in the HA-treated columns sharply dropped to below its MCL, and decreased further to non-detectable levels (estimated minimum detection limit 0.001  $\mu$ M U for these samples by KPA), and remained non-detectable over 100 PV leaching during the course of  $\sim$ 200 days. It should be pointed out that even under the conditions of 10 times reduced flow rate and increased pH up to 6, the effluent U and HA concentrations remained non-

detectable, indicating the very strong adsorption. Note that the minimum detection limit of U (0.001  $\mu\text{M}$ ) was applied to plot all the non-detectable [U] values. In contrast, for the control columns, U continued to be leached out, particularly from the column with pH 3.5 influent. The effluent [U] was more sensitive to pH fluctuation during the earlier times when the U inventory in sediment was still high. Later on, effluent [U] in the control columns continued to decrease, reflecting reduction of sediment U inventory. Based on our measured U concentration in the original contaminated SRS sediment, the total released U concentrations from the control columns after 106 PV are 95% at pH 3.5 and 42% at pH 4.5. In strong contrast, only 1% and 2% of the original U were leached out of the HA-treated pH 3.5 and 4.5 columns, respectively.

**Application of HA In-Situ U Remediation.** The batch equilibrium experiments show that HA adsorption onto sediment surfaces is quick, strong and practically irreversible at  $\text{pH} < 5.0$ . The mineral-adsorbed HA strongly complexes and effectively immobilizes U(VI) under acidic conditions. The column experiments show that injection of HA to the contaminated SRS sediments caused rapid U immobilization. Subsequent leaching with 100 pore volumes of simulated groundwater over 200 days at pH 3.5 to 6.0 did not release detectable concentrations of U. These results demonstrated that HA-treatment has potential as an in-situ remediation method for immobilizing U(VI) in acidic plumes. As the proposed remediation reagents, HAs (refractory decomposition product of biological materials, dead plants and organisms) are very resistant to further biodegradation, and persistent in the environment (24, 32). HAs are non-toxic, abundantly extractable from many environments, and are water-soluble so that they can be easily introduced into the subsurface. Additional research is needed, including determining the effects of competing ions, such as  $\text{Ca}^{2+}$ ,  $\text{Mg}^{2+}$ ,  $\text{Al}^{3+}$ , and  $\text{NO}_3^-$ , which can occur at elevated

concentrations in some plumes. An in-situ field experiment needs to be conducted to further test this method.

### **Acknowledgements**

This work was supported by the Lawrence Berkeley National Laboratory's Exploratory Project Opportunity, as part of the Subsurface Science Scientific Focus Area (SFA) funded by the U.S. Department of Energy, Office of Science, Office of Biological and Environmental Resources under Award Number DE-AC02-05CH11231. We thank Dr. Miles Denham for providing us the sediment samples from the Savannah River Site. We appreciate the helpful comments from four anonymous reviewers and the associate editor Dr. Dzombak.

### **Supporting Information Available**

Detailed Materials and Methods section, Tables of chemical properties of HAs used, characterization of SRS sediments, HA and U adsorption kinetic modeling data, and Langmuir modeling data for HA sorption are available in SI. The figures for HA adsorption as function of pH, and the modeling results of U(VI) species distribution are also available in SI, free of charge via the Internet at <http://pubs.acs.org>.

### **Literature Cited.**

(1) Tokunaga, T. K.; Wan, J.; Kim, Y.; Daly, R. A.; Brodie, E. L.; Hazen, T. C.; Herman, D.; Firestone, M. K., Influences of Organic Carbon Supply Rate on Uranium Bioreduction in Initially Oxidizing, Contaminated Sediment. *Environ. Sci. Technol.* **2008**, *42*, (23), 8901-8907.

- (2) Wan, J.; Tokunaga, T. K.; Brodie, E.; Wang, Z.; Zheng, Z.; Herman, D.; Hazen, T. C.; Firestone, M. K.; Sutton, S. R., Reoxidation of bio-reduced uranium under reducing conditions. *Environ. Sci. Technol.* **2005**, *39*, (16), 6162-6169.
- (3) Wan, J.; Tokunaga, T. K.; Kim, Y.; Brodie, E.; Daly, R.; Hazen, T. C.; Firestone, M. K., Effects of Organic Carbon Supply Rates on Uranium Mobility in a Previously Bio-reduced Contaminated Sediment. *Environ. Sci. Technol.* **2008**, *42*, (20), 7573-7579.
- (4) Wu, W.; Carley, J.; Fienen, M.; Mehlhorn, T.; Lowe, K.; Nyman, J.; Luo, J.; Gentile, M. E.; Rajan, R.; Wagner, D.; Hickey, R. F.; Gu, B.; Watson, D.; Cirpka, O. A.; Kitanidis, P. K.; Jardine, P. M.; Criddle, C. S., Pilot-scale in situ bioremediation of uranium in a highly contaminated aquifer. 1. Conditioning of a treatment zone. *Environ. Sci. Technol.* **2006**, *40*, (12), 3978-3985.
- (5) Tokunaga, T. K.; Kim, Y.; Wan, J., Potential Remediation Approach for Uranium-Contaminated Groundwaters Through Potassium Uranyl Vanadate Precipitation. *Environ. Sci. Technol.* **2009**, *43*, (14), 5467-5471.
- (6) Schnitzer, M., *Humic Substances: Chemistry and Reactions*. Elsevier Scientific Publishing Company: Amsterdam, 1978; Vol. Developments in Soil Science 8, p 319.
- (7) Stevenson, F. J., *Humus Chemistry: Genesis, Composition, Reactions*. John Wiley & Sons, Inc.: New York, 1994.
- (8) Gu, B.; Schmitt, J.; Chen, Z.; Liang, L.; McCarthy, J. F., Adsorption and desorption of different organic-matter fractions on iron-oxide. *Geochim. Cosmochim. Acta* **1995**, *59*, (2), 219-229.
- (9) Murphy, E. M.; Zachara, J. M., The role of sorbed humic substances on the distribution of organic and inorganic contaminants in groundwater. *Geoderma* **1995**, *67*, (1-2), 103-124.



- (10) Weng, L.; Van Riemsdijk, W. H.; Koopal, L. K.; Hiemstra, T., Adsorption of humic substances on goethite: Comparison between humic acids and fulvic acids. *Environ. Sci. Technol.* **2006**, *40*, (24), 7494-7500.
- (11) Choppin, G. R., Humics and radionuclide migration. *Radiochim. Acta* **1988**, *44-5*, 23-28.
- (12) Choppin, G. R., The role of natural organics in radionuclide migration in natural aquifer systems. *Radiochim. Acta* **1992**, *58-9*, 113-120.
- (13) Spirakis, C. S., The roles of organic matter in the formation of uranium deposits in sedimentary rocks. *Ore Geol. Rev.* **1996**, *11*, (1-3), 53-69.
- (14) Wood, S. A., The role of humic substances in the transport and fixation of metals of economic interest (Au, Pt, Pd, U, V). *Ore Geol. Rev.* **1996**, *11*, (1-3), 1-31.
- (15) Davis, J. A., Complexation of trace-metals by adsorbed natural organic-matter. *Geochim. Cosmochim. Acta* **1984**, *48*, (4), 679-691.
- (16) Gu, B.; Schmitt, J.; Chen, Z.; Liang, L.; McCarthy, J. F., Adsorption and desorption of natural organic-matter on iron-oxide - Mechanisms and models. *Environ. Sci. Technol.* **1994**, *28*, (1), 38-46.
- (17) Dong, W.; Xie, G.; Miller, T. R.; Franklin, M. P.; Oxenberg, T. P.; Bouwer, E. J.; Ball, W. P.; Halden, R. U., Sorption and bioreduction of hexavalent uranium at a military facility by the Chesapeake Bay. *Environ. Pollution* **2006**, *142*, (1), 132-142.
- (18) Krepelova, A.; Sachs, S.; Bernhard, G., Uranium(VI) sorption onto kaolinite in the presence and absence of humic acid. *Radiochim. Acta* **2006**, *94*, (12), 825-833.
- (19) Payne, T. E.; Davis, J. A.; Waite, T. D., Uranium adsorption on ferrihydrite - Effects of phosphate and humic acid. *Radiochimica Acta* **1996**, *74*, 239-243.

- (20) Artinger, R.; Rabung, T.; Kim, J. I.; Sachs, S.; Schmeide, K.; Heise, K. H.; Bernhard, G.; Nitsche, H., Humic colloid-borne migration of uranium in sand columns. *J. Contam. Hydrol.* **2002**, *58*, (1-2), 1-12.
- (21) Lenhart, J. J.; Honeyman, B. D., Uranium(VI) sorption to hematite in the presence of humic acid. *Geochim. Cosmochim. Acta* **1999**, *63*, (19-20), 2891-2901.
- (22) Kretzschmar, R.; Hesterberg, D.; Sticher, H., Effects of adsorbed humic acid on surface charge and flocculation of kaolinite. *Soil Sci. Soc. Am. J.* **1997**, *61*, (1), 101-108.
- (23) Tipping, E.; Griffith, J. R.; Hilton, J., The effect of adsorbed humic substances on the uptake of copper(II) by goethite. *Croat. Chem. Acta* **1983**, *56*, (4), 613-621.
- (24) Tipping, E., *Cation Binding by Humic Substances*. Cambridge University: 2002; p 434.
- (25) Zheng, Z.; Tokunaga, T. K.; Wan, J., Influence of calcium carbonate on U(VI) sorption to soils. *Environ. Sci. Technol.* **2003**, *37*, (24), 5603-5608.
- (26) Arda, D.; Hizal, J.; Apak, R., Surface complexation modelling of uranyl adsorption onto kaolinite based clay minerals using FITEQL 3.2. *Radiochim. Acta* **2006**, *94*, (12), 835-844.
- (27) Aquino, A. J. A.; Tunega, D.; Haberhauer, G.; Gerzabek, M. H.; Lischka, H., Acid-base properties of a goethite surface model: A theoretical view. *Geochim. Cosmochim. Acta* **2008**, *72*, (15), 3587-3602.
- (28) Sherman, D. M.; Peacock, C. L.; Hubbard, C. G., Surface complexation of U(VI) on goethite (alpha-FeOOH). *Geochim. Cosmochim. Acta* **2008**, *72*, (2), 298-310.
- (29) Parfitt, R. L.; Fraser, A. R.; Farmer, V. C., Adsorption on hydrous oxides .3. Fulvic-acid and humic-acid on goethite, gibbsite and imogolite. *J. Soil Sci.* **1977**, *28*, (2), 289-296.
- (30) Shinozuka, T.; Shibata, M.; Yamaguchi, T., Molecular weight characterization of humic substances by MALDI-TOF-MS. *J. Mass Spectrom. Soc. Jpn.* **2004**, *52*, (1), 29-32.

(31) Wang, K.; Xing, B., Structural and sorption characteristics of adsorbed humic acid on clay minerals. *J. Environ. Qual.* **2005**, *34*, (1), 342-349.

(32) Abbt-Braun, G.; Lankes, U.; Frimmel, F. H., Structural characterization of aquatic humic substances - The need for a multiple method approach. *Aquat. Sci.* **2004**, *66*, (2), 151-170.

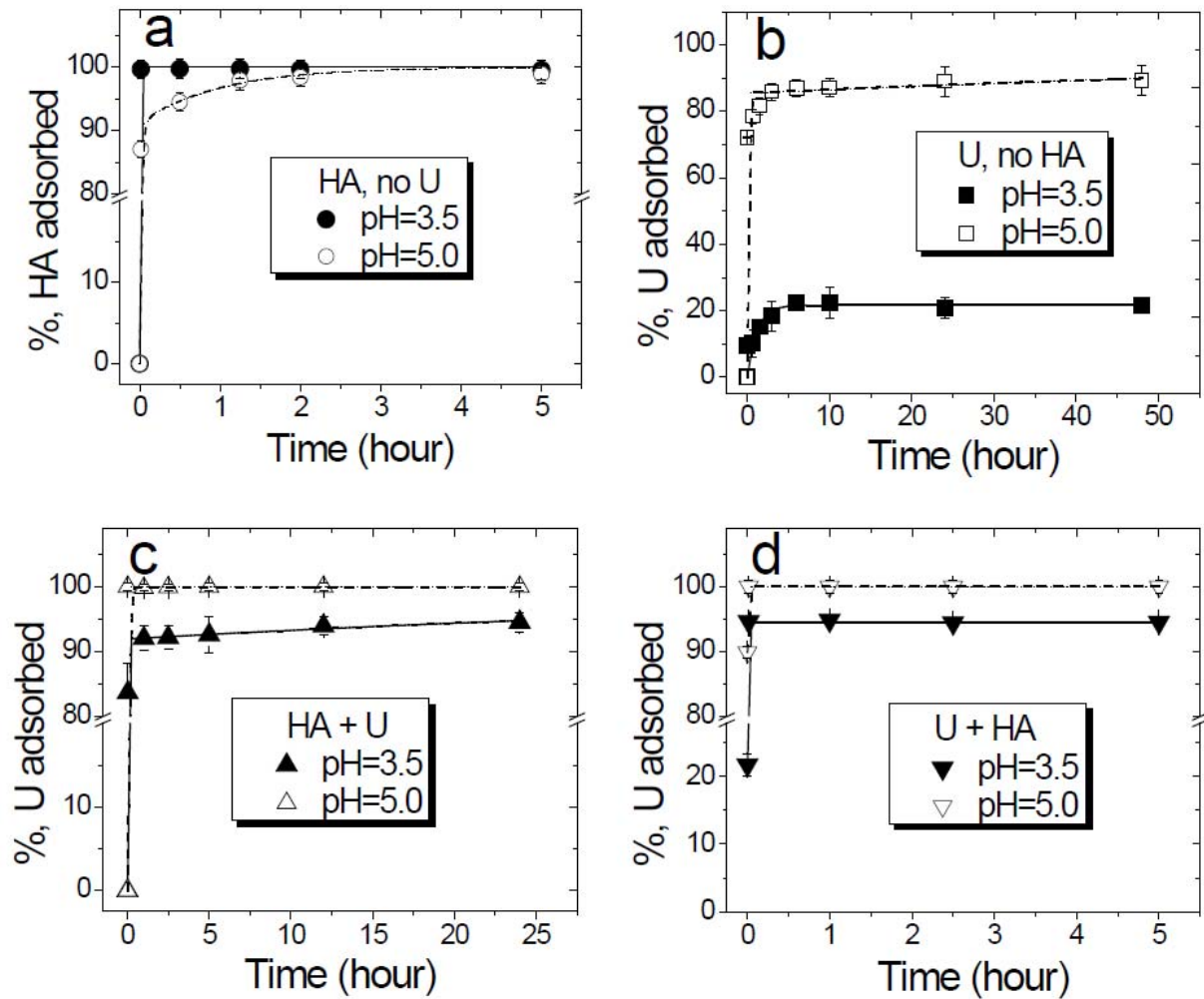


**Figure 1.** Adsorption rate and extent of Soil HA and U onto the fine-fraction of background SRS sediment under conditions of 5 g solid /L, 0.01M NaNO<sub>3</sub>, initial 50 mg HA/L, initial 1 μM U, atmospheric CO<sub>2</sub> (10<sup>-3.5</sup> atm), and ambient temperature (22.5 °C). (a) HA adsorption without U; (b) U adsorption without HA; (c) U adsorption after HA-reacted with the sediment for 48 hours; (d) U adsorption enhanced by adding HA to the sediment that has been pre-reacted with U for 48 hours. Symbols are experimental data points from the mean of duplicate samples with standard deviation. The solid and dashed lines are the modeled data with pseudo-first-order rate reaction (see Table S-3 in SI).

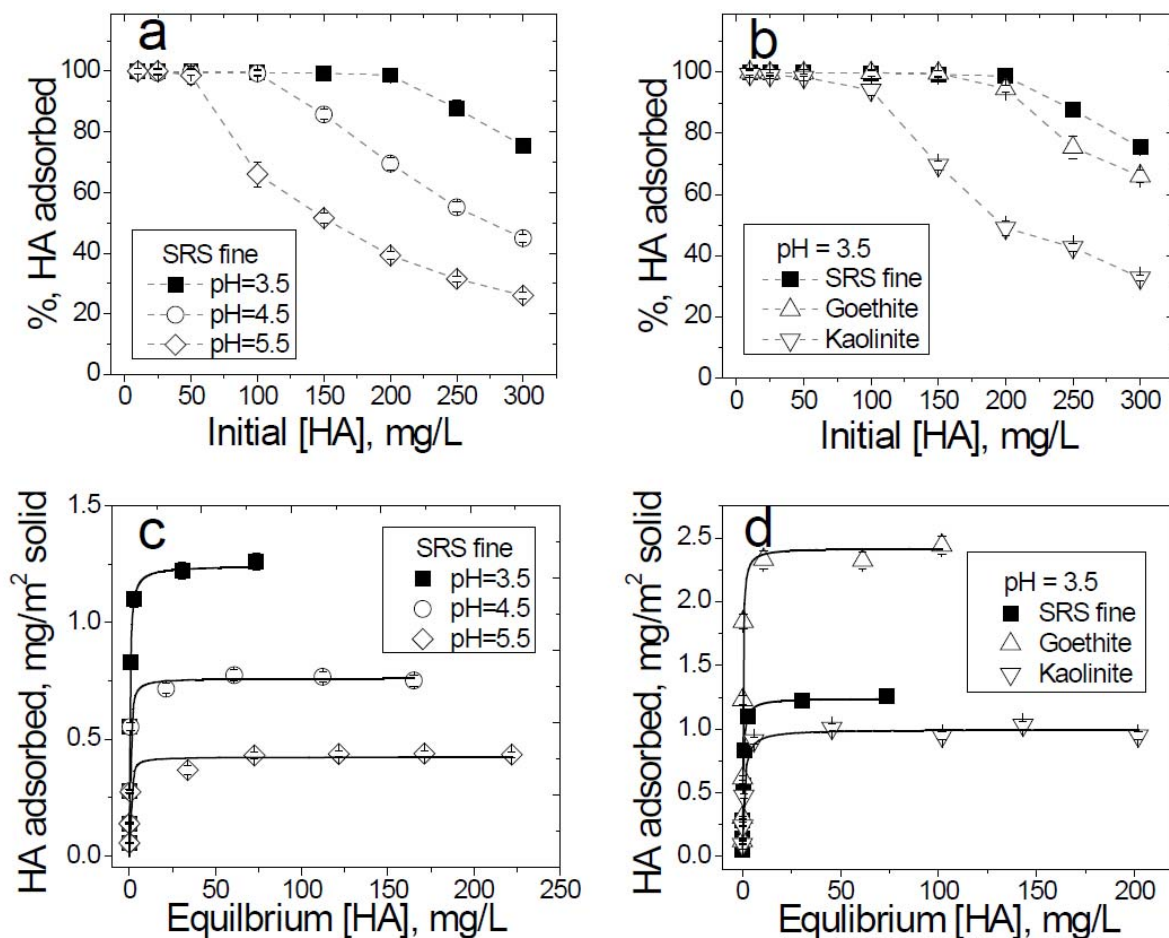


**Figure 2.** HA adsorption percentages (a, b) and isotherms (c, d), under conditions of 5 g solid /L, 0.01M NaNO<sub>3</sub>, atmospheric CO<sub>2</sub> (10<sup>-3.5</sup> atm) and ambient temperature (22.5 °C). (a) HA adsorption percentage onto SRS fine-fraction as function of initial HA concentration at different pH; (b) HA adsorption percentage onto three different sorbents as function of initial HA concentration at pH 3.5; (c) HA adsorption isotherms onto SRS fine-fraction at different pH; (d) HA adsorption isotherms for three different sorbents at pH 3.5. Symbols are experimental data representing a mean of duplicate samples with standard deviation bars. Dashed-lines in (a, b) indicate data trends, and solid lines in (c, d) are Langmuir modeling results (details in Table S-4 in SI).

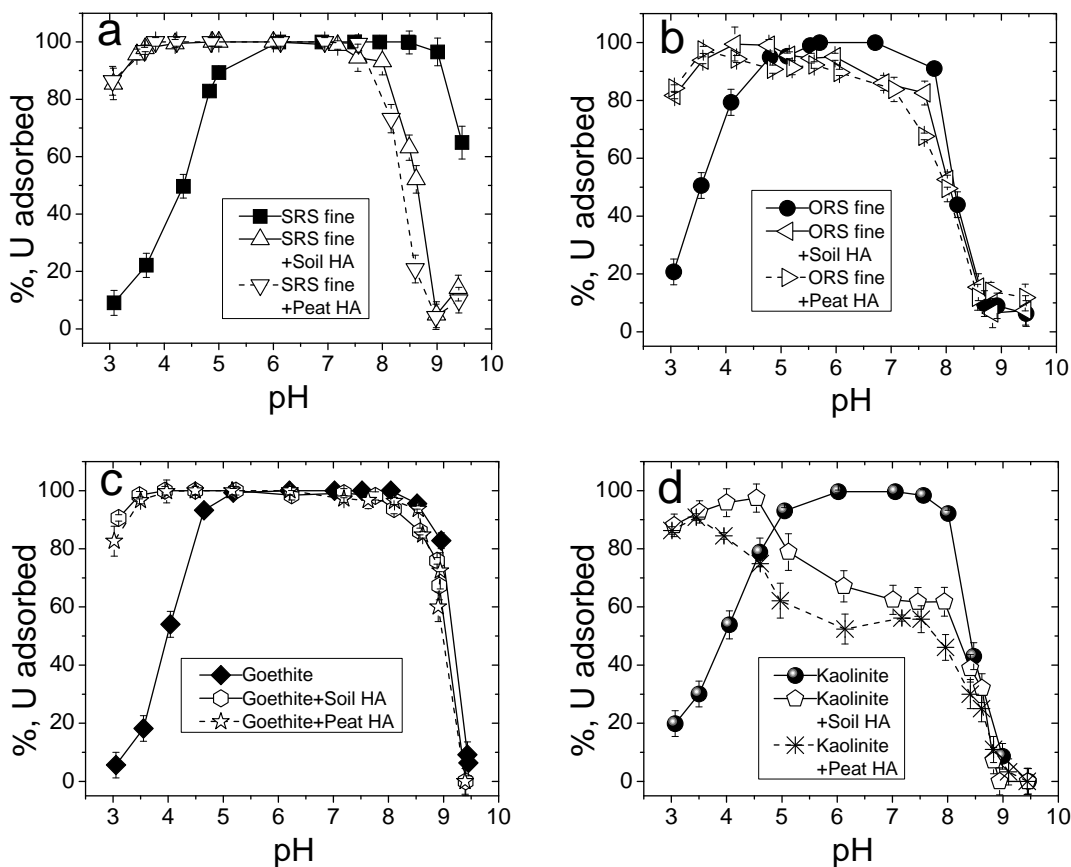


**Figure 3.** Impact of HA on U(VI) adsorption as function of pH onto (a) SRS fine-fraction, (b) ORS fine-fraction, (c) goethite, and (d) kaolinite, in absence and presence of 50 mg/L of soil-HA or peat-HA under conditions of solid concentration 5 g/L, initial 1.0  $\mu\text{M}$  U, 0.01M  $\text{NaNO}_3$ , atmospheric  $\text{CO}_2$  ( $10^{-3.5}$  atm) and ambient temperature ( $22.5^\circ\text{C}$ ). Symbols are experimental data points from means of duplicate samples with standard deviation bars, and solid and dashed lines show the data trends.

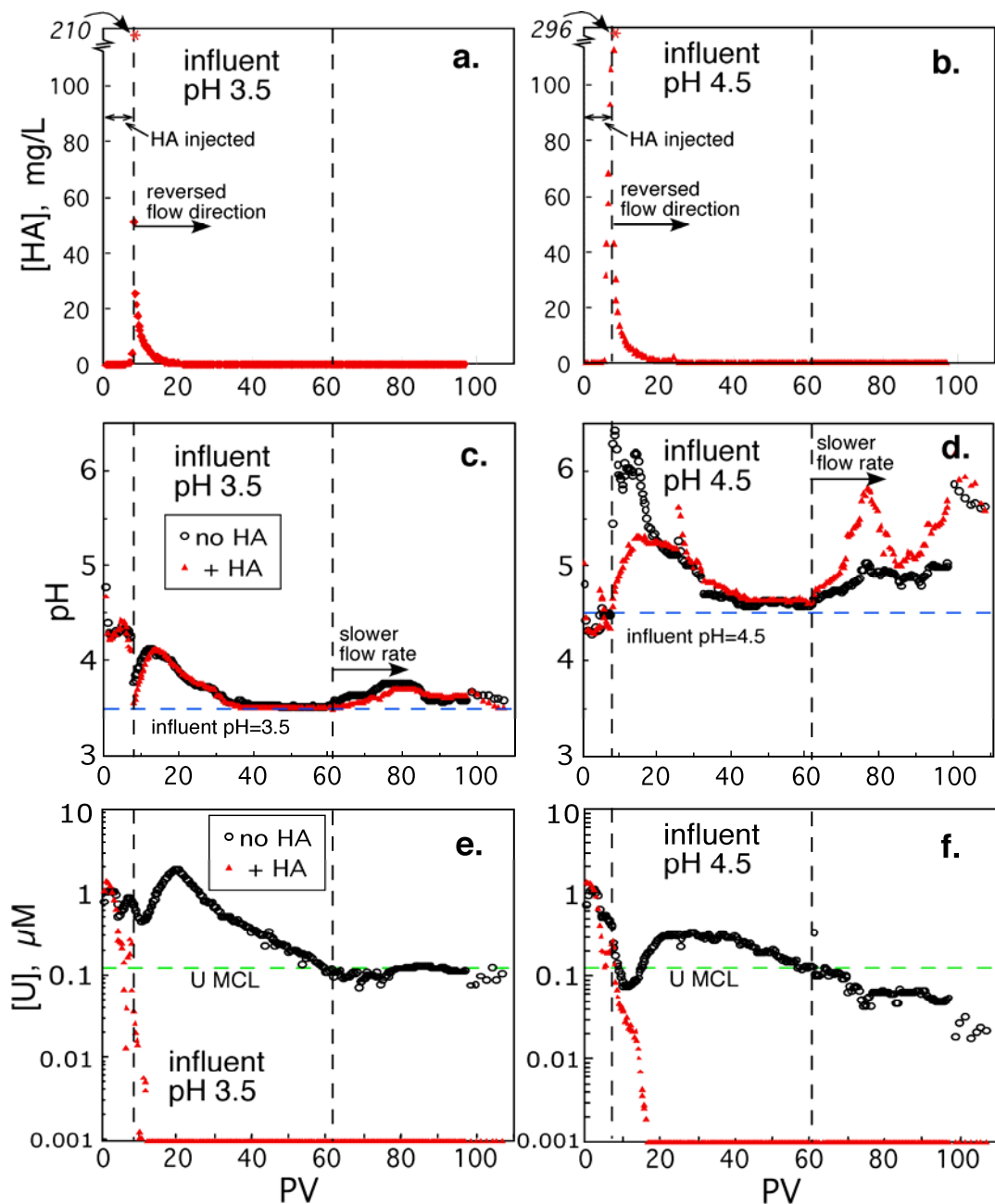


**Figure 4.** Breakthrough curves of [U] and [HA], and pH show that HA treatment significantly enhanced U immobilization in SRS contaminated sediment columns under acidic leaching conditions: pH 3.5 (a, c, e) and pH 4.5 (b, d, f). The vertical dashed-lines at PV 7.9 indicate the transition point from HA injecting/treatment to simulated groundwater leaching under reverse flow direction. All influent solutions contain 0.01M NaNO<sub>3</sub>. Dashed-lines at PV 60 indicate the point of flow rate change from 120 m/y to 12 m/y.

## **DISCLAIMER**

This document was prepared as an account of work sponsored by the United States Government. While this document is believed to contain correct information, neither the United States Government nor any agency thereof, nor the Regents of the University of California, nor any of their employees, makes any warranty, express or implied, or assumes any legal responsibility for the accuracy, completeness, or usefulness of any information, apparatus, product, or process disclosed, or represents that its use would not infringe privately owned rights. Reference herein to any specific commercial product, process, or service by its trade name, trademark, manufacturer, or otherwise, does not necessarily constitute or imply its endorsement, recommendation, or favoring by the United States Government or any agency thereof, or the Regents of the University of California. The views and opinions of authors expressed herein do not necessarily state or reflect those of the United States Government or any agency thereof or the Regents of the University of California.